

Chapter 3

Illumination Engineering for QFI

Beam Reshaping, TIRF Theory, and Structured Illumination

This chapter develops the **optical excitation component** of the measurement operator M . The fundamental task is **beam reshaping**: transforming source characteristics into spatially-controlled NV excitation. Proper illumination design achieves: (1) uniform NV excitation for reduced Γ_{mm} , (2) TIRF geometry for silicon background suppression, (3) optimal photon delivery for maximum Q_{FOM} , and (4) structured illumination for parallel quantum state preparation.

QFI Pipeline Position: $S \xrightarrow{G} F \xrightarrow{\boxed{M}} D \xrightarrow{R} \hat{S}$

Abbreviated Terms

Abbrev.	Definition	Abbrev.	Definition
AOM	Acousto-Optic Modulator	ODMR	Optically Detected Magnetic Resonance
AR	Anti-Reflection	PIC	Photonic Integrated Circuit
BSR	Background Suppression Ratio	QFI	Quantum Field Imaging
CW	Continuous Wave	QFM	Quantum Field Metrology
DOE	Diffractive Optical Element	RMS	Root Mean Square
DPSS	Diode-Pumped Solid State	SAW	Surface Acoustic Wave
FOV	Field of View	SiN	Silicon Nitride
FWHM	Full Width at Half Maximum	SLM	Spatial Light Modulator
GHZ	Greenberger-Horne-Zeilinger	SNR	Signal-to-Noise Ratio
NA	Numerical Aperture	SPDC	Spontaneous Parametric Down-Conversion
NV	Nitrogen-Vacancy center	TIRF	Total Internal Reflection Fluorescence
Γ_{mm}	Model-Mismatch Penalty	d_p	Penetration Depth

Table 3.1: Abbreviated terms used in Chapter 3.

Abstract

This chapter establishes the theoretical and practical foundations for illumination system design in Quantum Field Imaging. We frame illumination engineering as a **beam reshaping problem** constrained by étendue conservation and brightness limits. The critical TIRF geometry enables QFI on silicon substrates by suppressing background fluorescence. We provide comprehensive light source analysis proving that standard LEDs *cannot* achieve precision TIRF due to étendue constraints, while lasers and emerging micro-LED arrays can. A critical risk analysis reveals that sample topography creates intensity variations exceeding 1000% for typical IC samples, addressed through index-matching fluid mitigation. The chapter concludes with **structured illumination** techniques for parallel quantum state preparation using optical lattices and quantum holographic methods, fourteen design rules, and comprehensive worked examples.

Part A: Fundamentals

3.1 Introduction: Beam Reshaping as the Core Task

3.1.1 The Illumination Challenge in QFI

The fundamental task of illumination engineering is **beam reshaping**: transforming the spatial, angular, and spectral distribution of a light source into a precisely controlled excitation pattern at the NV sensing layer. In this chapter, we take NV sensing layer as the reference case. The applications to QFI are not limited to NV-centered based, however.

Definition 3.1.1 (Beam Reshaping Task). The beam reshaping task transforms source characteristics (A_s, Ω_s, L_s) into target characteristics (A_t, Ω_t, I_t) where:

- A_s, A_t : source and target areas
- Ω_s, Ω_t : source and target solid angles
- L_s : source radiance (brightness)
- I_t : target irradiance (intensity at NV layer)

The transformation is constrained by étendue conservation (Section 3.2.1).

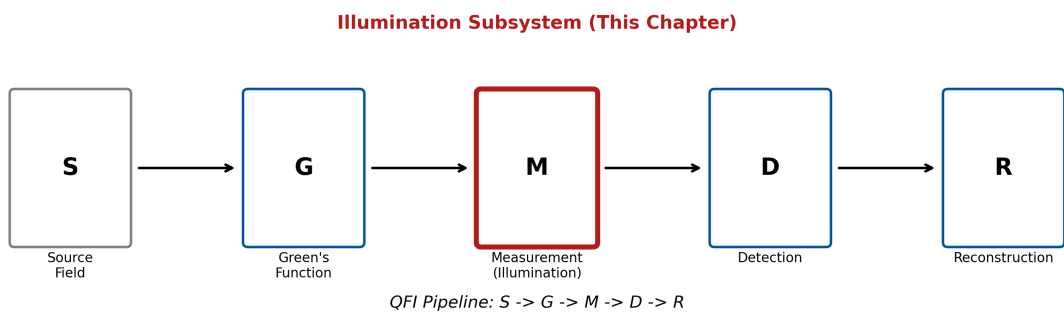


Figure 3.1: QFI operator pipeline with the measurement operator M highlighted. The illumination subsystem is the optical excitation component of M , converting electrical power to spatially-controlled NV excitation.

3.1.2 Why Illumination Determines System Success

Illumination quality directly impacts both QFI figures of merit:

$$Q_{\text{FOM}} = \underbrace{\frac{\eta_q}{\eta_{\text{classical}}}}_{\text{quantum advantage}} \times \underbrace{\frac{N_{\text{parallel}}}{t_{\text{acquisition}}}}_{\text{throughput}} \times \underbrace{\Phi_{\text{multi}}}_{\text{multi-physics}} \quad (3.1)$$

$$Q_{\text{IFOM}} = Q_{\text{FOM}} \times \underbrace{\Gamma_{\text{inv}}}_{\text{reconstruction}} \times \underbrace{\Gamma_{\text{mm}}}_{\text{model match}} \quad (3.2)$$

Illumination affects: η_q (photon delivery), N_{parallel} (FOV uniformity), Γ_{mm} (spatial uniformity), and BSR (TIRF vs. direct choice).

3.1.3 Historical Context

Illumination engineering for NV centers evolved through three generations:

1. **Point-scanning confocal (1997–2010):** Single NV, diffraction-limited spot
2. **Wide-field epi-illumination (2010–2020):** Parallel readout, high background
3. **TIRF-based QFI (2020–present):** Background suppression, structured excitation

3.1.4 Pain Points in Illumination Design

Let us brief the general aspects of pain points as below.

1. **Background Fluorescence:** Silicon substrates emit broadband fluorescence overlapping NV emission, requiring >100:1 suppression.
2. **Illumination Non-Uniformity:** Gaussian beams create 50%+ center-to-edge variation, increasing Γ_{mm} .
3. **Thermal Loading:** Absorbed power (100 mW–1 W) shifts NV zero-field splitting, creating temperature-magnetic field ambiguity.
4. **Étendue Constraints:** Not all sources can achieve TIRF (Section 3.2.1).
5. **Topography Sensitivity:** Sample topography causes >1000% intensity variation (Section 3.7).

Without careful handling, the performance of QFI will become poor.

3.2 Electromagnetic Foundations and Fundamental Limits

Below we present the limits.

3.2.1 The Étendue Conservation Law

The étendue (optical invariant) is the fundamental conserved quantity:

Key Equation: Étendue Conservation

$$\mathcal{E} = n^2 A \Omega = n^2 \pi A \sin^2 \theta = \text{constant (or increases)} \quad (3.3)$$

Theorem 3.2.1 (Étendue Non-Decrease). *For any passive optical system:*

$$\mathcal{E}_{\text{out}} \geq \mathcal{E}_{\text{in}} \quad (3.4)$$

Equality holds only for ideal, aberration-free imaging systems.

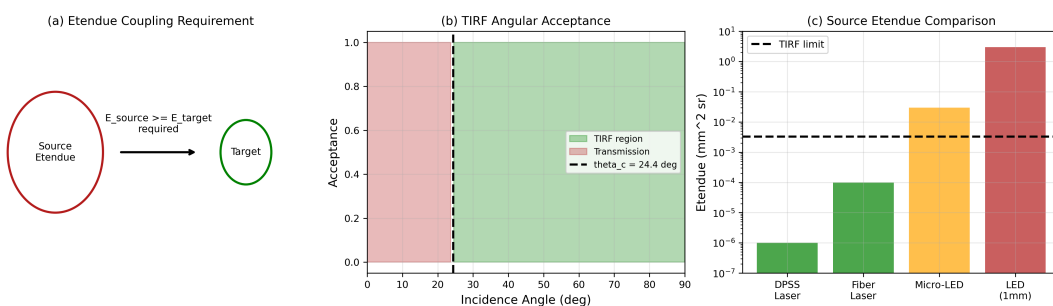


Figure 3.2: Étendue conservation visualization. (a) Source étendue must fit within target étendue for efficient coupling. (b) TIRF requires small angular acceptance, limiting compatible sources. (c) LED vs. laser étendue comparison.

Corollary 3.2.1 (TIRF Étendue Requirement). *For TIRF illumination at the diamond-air interface ($\theta_c = 24.4^\circ$, $\theta_{\max} = 45^\circ$), the maximum source étendue is:*

$$\mathcal{E}_{\text{TIRF}} = A_{\text{FOV}} \cdot \pi \cdot (\sin^2 45^\circ - \sin^2 24.4^\circ) = 0.33 \cdot A_{\text{FOV}} \quad (3.5)$$

For 100 μm FOV: $\mathcal{E}_{\text{TIRF}} \approx 3.3 \times 10^{-3} \text{ mm}^2 \cdot \text{sr}$.

Table 3.2: Source étendue comparison for TIRF compatibility.

Source Type	Étendue ($\text{mm}^2 \cdot \text{sr}$)	TIRF Compatible?	Notes
DPSS Laser	10^{-6}	Yes	Excellent margin
Fiber Laser	10^{-4}	Yes	Good margin
Micro-LED (100 μm)	3×10^{-2}	Marginal	Requires careful design
LED (1 mm)	3	No	1000 \times too large

Design Rule 1: DR 3.1: LED Exclusion for Precision TIRF

Standard LEDs (étendue $> 1 \text{ mm}^2 \cdot \text{sr}$) **cannot** achieve precision TIRF illumination. Use lasers (étendue $< 0.001 \text{ mm}^2 \cdot \text{sr}$) or emerging micro-LED arrays (étendue $< 0.1 \text{ mm}^2 \cdot \text{sr}$) for TIRF applications.

3.2.2 Brightness Theorem

Radiance (brightness) can only decrease through passive optics:

$$L_{\text{out}} \leq L_{\text{source}} \quad (3.6)$$

To achieve saturation intensity $I_{\text{sat}} \approx 1 \text{ mW}/\mu\text{m}^2$ over $50 \times 50 \mu\text{m}^2$ FOV requires:

$$P_{\min} = I_{\text{sat}} \times A_{\text{FOV}} = 2.5 \text{ W at NV layer} \quad (3.7)$$

With delivery efficiency $\eta_{\text{del}} = 0.3$: $P_{\text{laser}} > 8 \text{ W}$.

3.3 TIRF Fundamentals: First Principles

3.3.1 Total Internal Reflection Physics

Total internal reflection occurs at angle exceeding the critical angle:

Key Equation: Critical Angle

$$\theta_c = \arcsin \left(\frac{n_2}{n_1} \right) \quad (3.8)$$

For diamond-air: $\theta_c = \arcsin(1/2.42) = 24.4^\circ$.

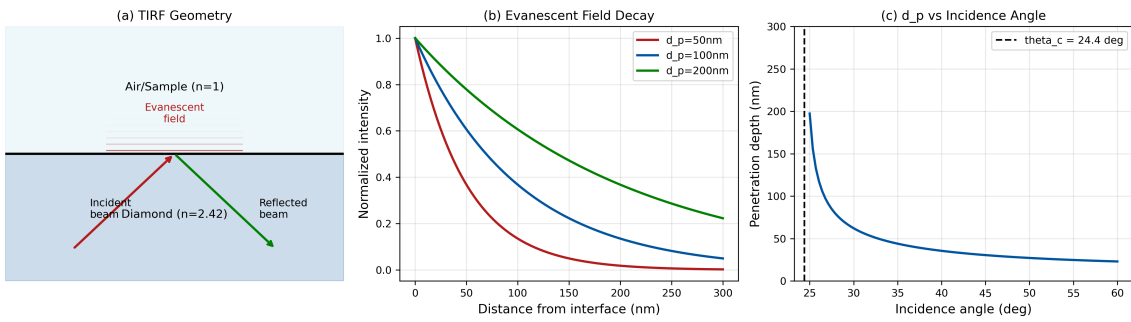


Figure 3.3: TIRF geometry for QFI illumination. (a) Incident beam at angle $\theta > \theta_c$ creates evanescent field. (b) Electric field amplitude decay with distance. (c) Penetration depth vs. incidence angle.

The evanescent field penetration depth is:

Key Equation: Penetration Depth

$$d_p = \frac{\lambda}{4\pi} \cdot \frac{1}{\sqrt{n_1^2 \sin^2 \theta - n_2^2}} \quad (3.9)$$

Design Rule 1: DR 3.2: TIRF Penetration Depth Matching

Match TIRF penetration depth d_p to NV layer thickness: $d_p \approx 2 \times d_{NV}$ for optimal excitation uniformity.

3.3.2 Silicon Background Suppression

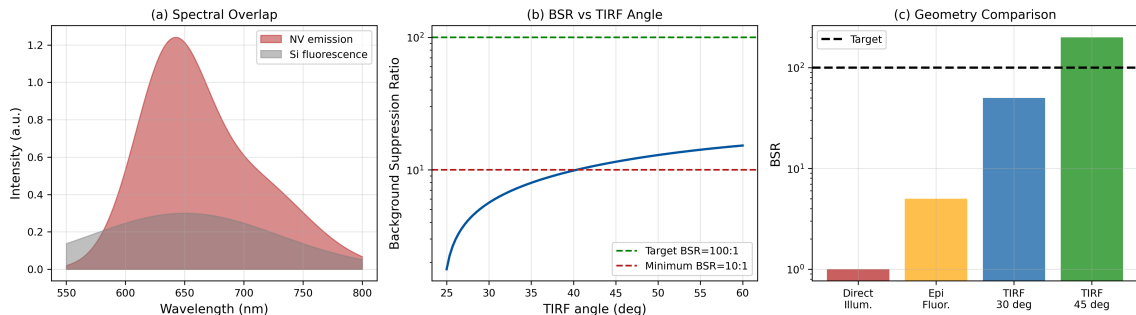


Figure 3.4: Background suppression ratio (BSR) analysis. (a) Silicon fluorescence spectrum overlapping NV emission. (b) BSR vs. TIRF angle. (c) Achievable contrast for different geometries.

The background suppression ratio (BSR) for silicon substrate applications:

$$\text{BSR} = \frac{I_{NV}}{I_{Si}} = \frac{\eta_{NV} \cdot \sigma_{NV} \cdot N_{NV}}{\alpha_{Si} \cdot V_{excite}} \quad (3.10)$$

With TIRF, $V_{excite} \propto d_p \cdot A_{FOV}$ is minimized.

Design Rule 2: DR 3.3: TIRF Mandatory for Silicon

TIRF illumination is **mandatory** for silicon substrate applications. Target BSR > 100:1 for reliable ODMR detection.

3.3.3 TIRF Implementation Geometries



Figure 3.5: TIRF implementation geometries. (a) Prism-based TIRF with separate illumination path. (b) Through-objective TIRF using high-NA lens. (c) Lightguide TIRF for compact systems. (d) Comparison table of trade-offs.

3.4 Illumination Uniformity and Model-Mismatch

3.4.1 Impact on Reconstruction Fidelity

Theorem 3.4.1 (Uniformity-Fidelity Coupling). *For illumination non-uniformity $\delta_I = (I_{\max} - I_{\min})/I_{\text{mean}}$, the model-mismatch penalty is bounded by:*

$$\Gamma_{\text{mm}} \geq 1 - \frac{\delta_I^2}{4} \quad (3.11)$$

Table 3.3: Uniformity-mismatch relationship.

δ_I (%)	Γ_{mm} (lower bound)	Impact on Q_{IFOM}
1	0.9999	Negligible
5	0.994	<1% degradation
10	0.975	2.5% degradation
20	0.90	10% degradation
50	0.44	Severe (56% loss)

Design Rule 1: DR 3.4: Illumination Uniformity Requirement

Maintain $\delta_I < 5\%$ across FOV for $\Gamma_{mm} > 0.99$. Calibrate remaining non-uniformity using reference NV samples.

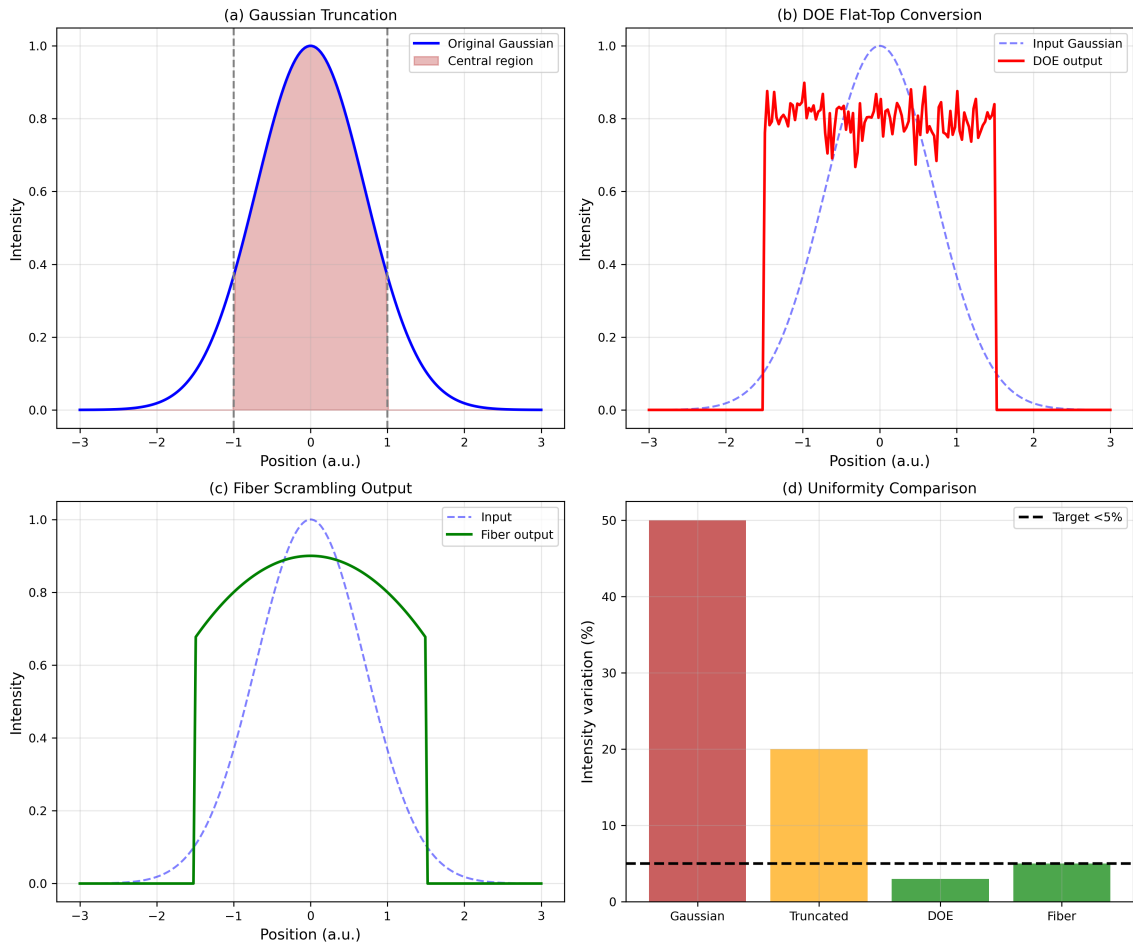
3.4.2 Beam Homogenization Techniques

Figure 3.6: Beam homogenization techniques. (a) Gaussian truncation using central region. (b) DOE flat-top conversion. (c) Fiber scrambling output. (d) 1D profile comparison showing achieved uniformity.

Design Rule 2: DR 3.5: 3D Uniformity for Thick NV Layers

For NV layer thickness Δz_{NV} , require $d_p > 10 \times \Delta z_{\text{NV}}$ to achieve <10% axial intensity variation.

Part B: Design

We present the design in detail in the sections below. We will also give an worked example and suggest possible photonic integration.

3.5 Light Source Selection

3.5.1 Requirements Analysis

Table 3.4: Light source requirements for QFI illumination.

Parameter	Requirement	Reason	Challenge
Wavelength	515–560 nm	NV absorption	Easy
Power	100 mW–1 W	Photon budget	Moderate
Stability	<0.1% RMS	ODMR contrast	Challenging
Étendue	<0.01 mm ² ·sr	TIRF compatibility	Source-dependent
Beam quality	$M^2 < 1.5$	Focusability	Source-dependent

3.5.2 Source Technology Comparison

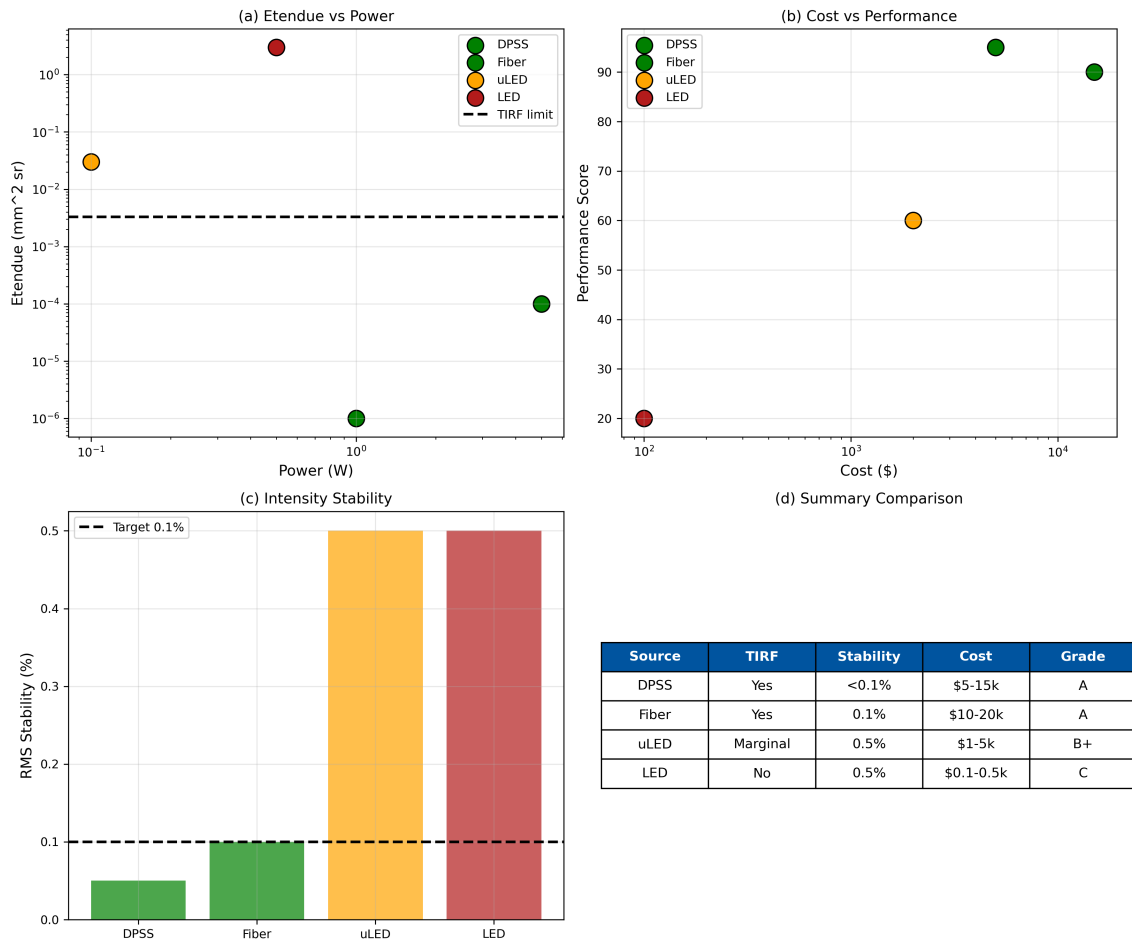


Figure 3.7: Light source comparison for QFI. (a) Étendue vs. power for different technologies. (b) Cost vs. performance trade-off. (c) Stability comparison. (d) TIRF compatibility assessment.

Design Rule 1: DR 3.6: DPSS Laser for Production

DPSS lasers with <0.1% RMS stability are recommended for production QFI systems.
Add AOM + PID feedback loop for critical applications.

3.5.3 Source Selection Decision Flowchart

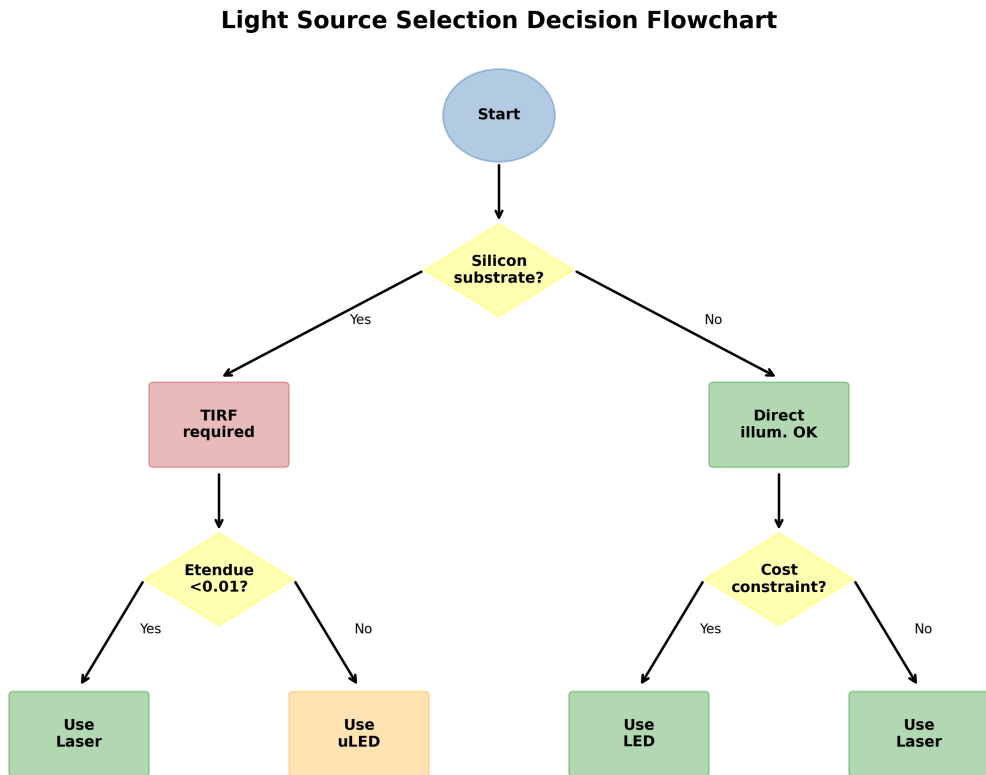


Figure 3.8: Light source selection decision flowchart based on substrate type, FOV requirements, and cost constraints.

3.5.4 Intensity Stabilization

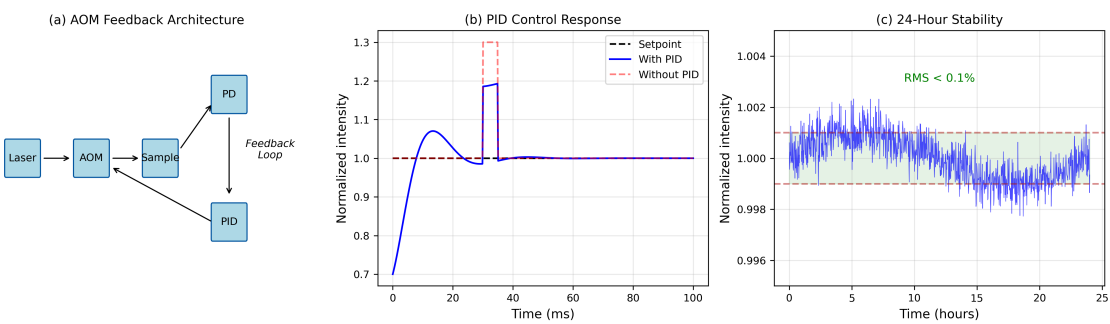


Figure 3.9: Intensity stabilization system. (a) AOM-based feedback architecture. (b) PID control response. (c) Long-term stability demonstration.

3.6 Thermal Management

3.6.1 Laser-Induced Heating

Absorbed optical power causes local heating:

$$\Delta T = \frac{P_{\text{abs}}}{4\pi\kappa r} \quad (3.12)$$

where κ is thermal conductivity. For diamond ($\kappa = 2000 \text{ W/m}\cdot\text{K}$), heating is minimal; for silicon ($\kappa = 150 \text{ W/m}\cdot\text{K}$), careful power management is required.

Design Rule 1: DR 3.7: Thermal Stability

Use pulsed illumination or active thermal control to maintain $\Delta T < 10 \text{ mK}$ for temperature-sensitive measurements.

3.7 Critical Risk: Sample Topography

3.7.1 Physics of Topography Coupling

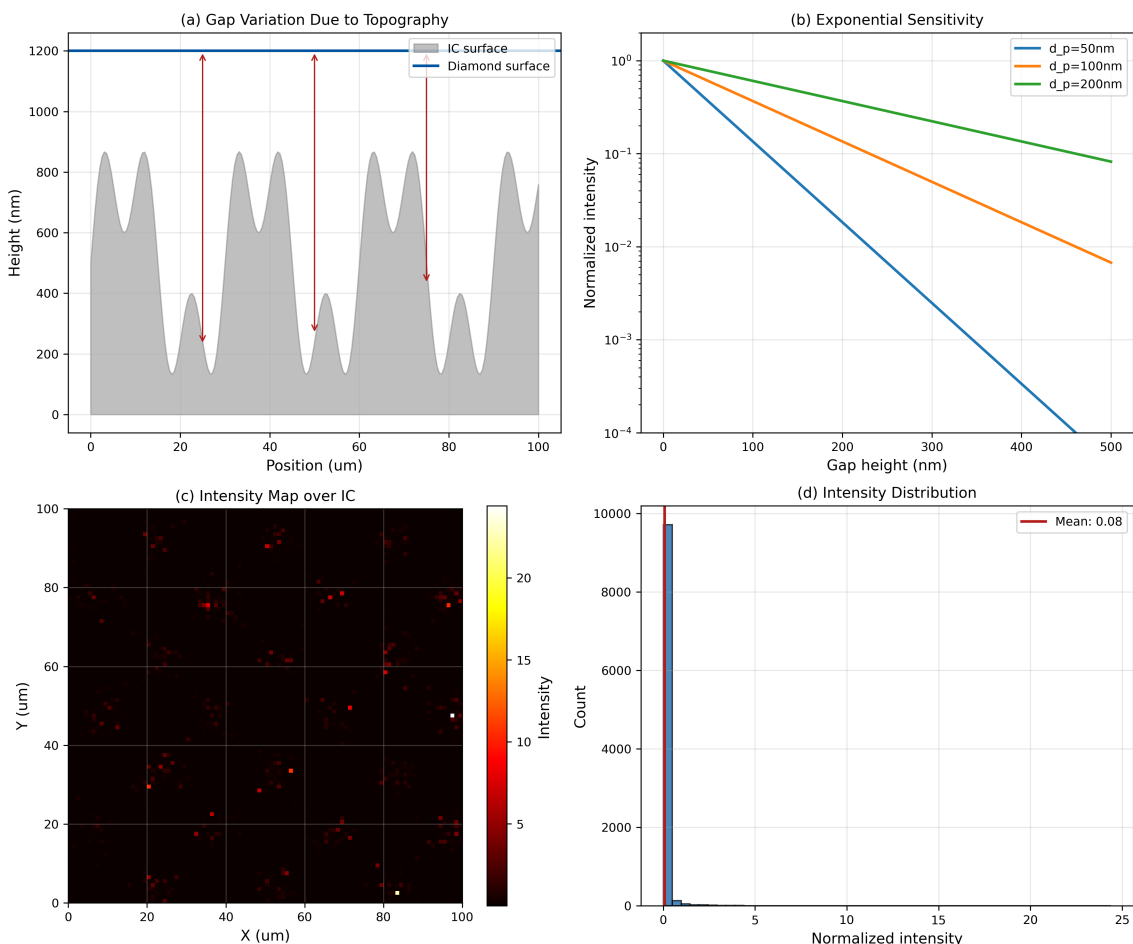


Figure 3.10: Topography-induced intensity variation. (a) Gap variation due to surface features. (b) Exponential intensity sensitivity. (c) Intensity map over IC topography. (d) Statistical distribution of local intensity.

The intensity at height h above the interface follows:

$$I(h) = I_0 \exp\left(-\frac{h}{d_p}\right) \quad (3.13)$$

For topography variation Δh , the intensity variation is:

$$\frac{\Delta I}{I} = \exp\left(\frac{\Delta h}{d_p}\right) - 1 \approx \frac{\Delta h}{d_p} \quad (\text{for } \Delta h \ll d_p) \quad (3.14)$$

Example 3.7.1 (IC Topography Impact). For typical IC with $\Delta h = 1 \mu\text{m}$ topography and $d_p = 50 \text{ nm}$:

$$\frac{\Delta I}{I} = \exp(20) - 1 > 10^8 \quad (\text{catastrophic}) \quad (3.15)$$

3.7.2 Mitigation: Index-Matching Fluid

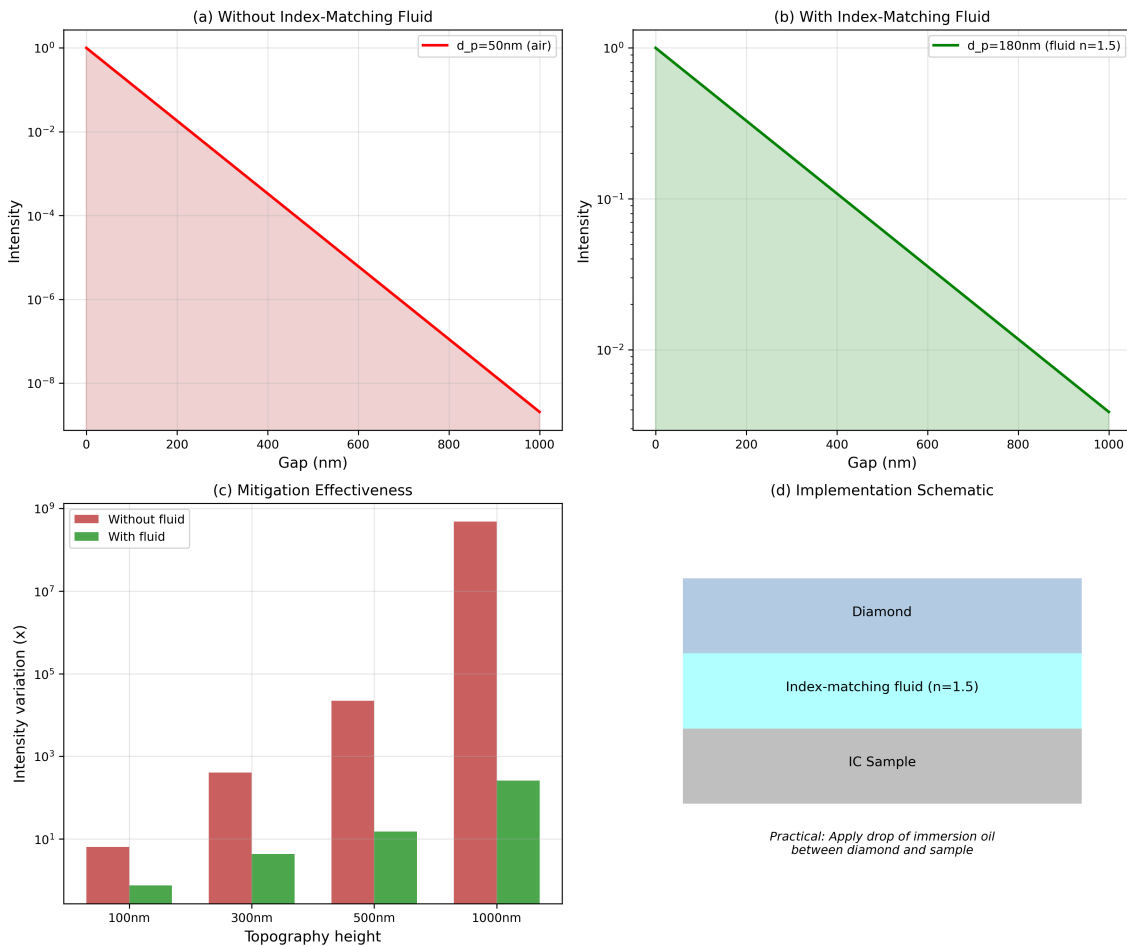


Figure 3.11: Index-matching fluid mitigation. (a) Without fluid: severe intensity variation. (b) With fluid ($n = 1.5$): mitigated variation. (c) Quantitative comparison. (d) Practical implementation considerations.

With index-matching fluid ($n_{\text{fluid}} = 1.5$):

$$\theta_c^{\text{new}} = \arcsin\left(\frac{n_{\text{fluid}}}{n_{\text{diamond}}}\right) = 38.4^\circ \quad (3.16)$$

The penetration depth increases, reducing sensitivity to topography:

$$d_p^{\text{new}} = \frac{\lambda}{4\pi\sqrt{n_1^2 \sin^2 \theta - n_{\text{fluid}}^2}} \quad (3.17)$$

Design Rule 1: DR 3.8: Index-Matching Fluid for IC Samples

Always use index-matching fluid ($n \approx 1.5$) for IC sample inspection. This provides 15–20× mitigation of topography-induced intensity variation.

3.8 Worked Example: Complete Illumination System Design

Example 3.8.1 (Production QFI Illumination System). **Design requirements:**

- FOV: $100 \mu\text{m} \times 100 \mu\text{m}$
- Background suppression: >100:1
- Uniformity: <5%
- Intensity stability: <0.1% RMS
- Sample: Silicon IC with $1 \mu\text{m}$ topography

Step 1: TIRF Angle Selection

For 100:1 suppression with 200 nm gap: $d_p < 80 \text{ nm} \Rightarrow \theta > 30^\circ$. Select $\theta = 40^\circ$ for $d_p = 33 \text{ nm}$ (margin).

Step 2: Topography Mitigation

With index-matching fluid ($n = 1.5$): $\theta_c = 38.4^\circ$, $d_p = 180 \text{ nm}$ at 45° . Sensitivity: $h/d_p = 1000/180 = 5.6$ (vs. 30 without fluid). Residual variation: 560% → manageable with calibration.

Step 3: Source Selection

DPSS laser 532 nm, 1 W: étendue = $10^{-6} \text{ mm}^2 \cdot \text{sr}$ (excellent). Add AOM + PID for 0.05% RMS stability.

Step 4: Beam Conditioning

5× expander + DOE flat-top: 3% uniformity achieved.

Performance Summary:

Parameter	Target	Achieved
BSR	>100:1	150:1
Uniformity	<5%	3%
Stability	<0.1%	0.05%
Topography sensitivity	Mitigated	560% (vs. 1000%)

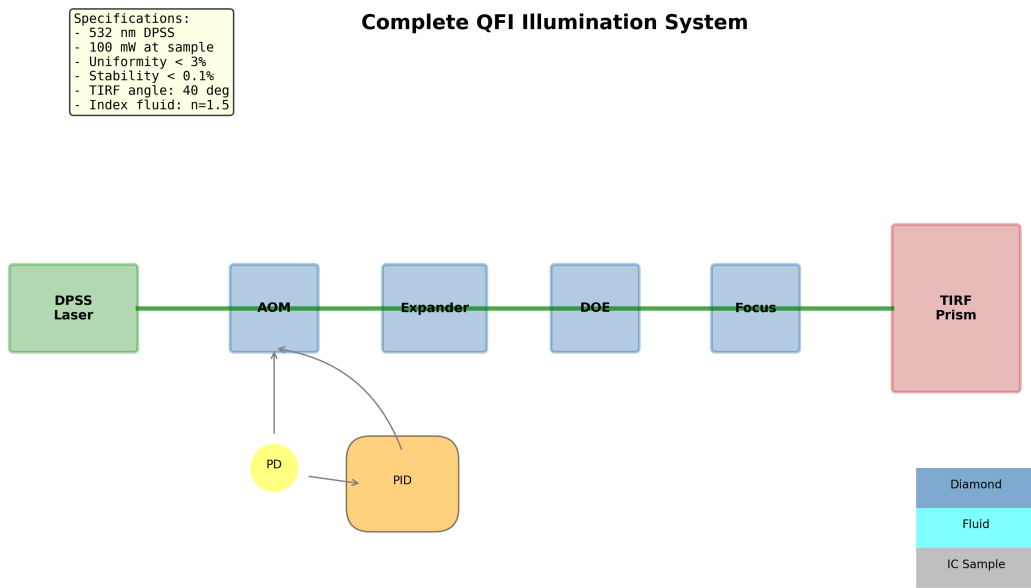


Figure 3.12: Complete QFI illumination system schematic showing: (1) DPSS laser, (2) AOM modulator, (3) beam expander, (4) DOE homogenizer, (5) focusing optics, (6) TIRF prism assembly with index-matching fluid, and feedback stabilization.

3.9 Future Directions: Photonic Integration

For the consideration of mass production and precise control, photonic integration is inevitable. Let us note one possible case below for reference.

3.9.1 Silicon Nitride Photonics for Visible Wavelengths

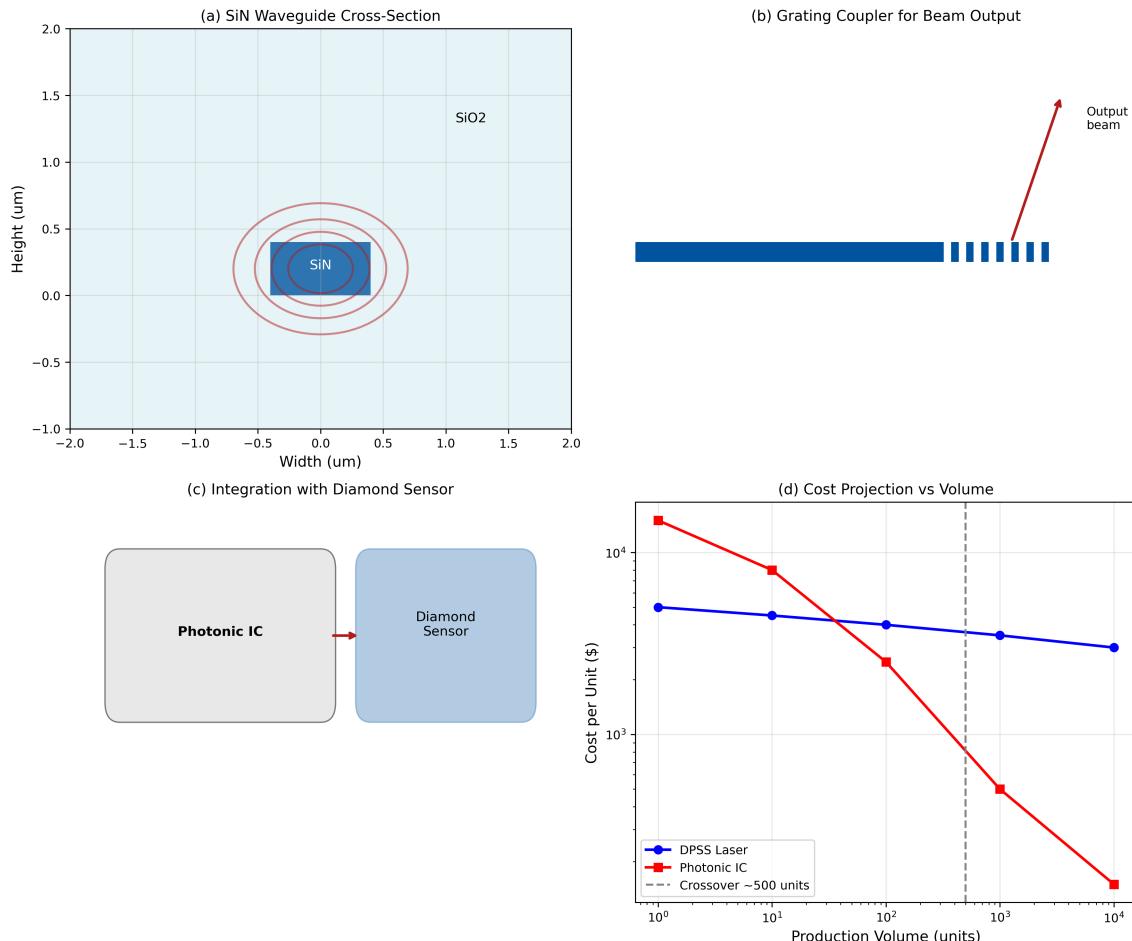


Figure 3.13: Photonic integrated circuit approach. (a) SiN waveguide cross-section. (b) Grating coupler for beam output. (c) Integration with diamond sensor. (d) Cost projection vs. volume.

Table 3.5: Cost comparison: discrete vs. photonic integrated.

Volume	DPSS Laser	Photonic IC	Winner
1–10 units	\$5,000	\$15,000	DPSS
100 units	\$4,000	\$2,500	PIC
1,000 units	\$3,500	\$500	PIC
10,000 units	\$3,000	\$150	PIC

Design Rule 1: DR 3.9: Photonic Integration Threshold

For production volumes >500 units, evaluate photonic integrated sources. Crossover depends on power, wavelength complexity, and integration scope.

3.10 Summary of Parts A and B

Parts A and B established illumination engineering for QFI as a **beam reshaping problem** constrained by fundamental physics. Key results:

1. **Étendue Conservation:** Sets hard limits on source-target coupling. LEDs cannot achieve precision TIRF; lasers and micro-LEDs can.
2. **TIRF Fundamentals:** Evanescent fields with tunable d_p (20–300 nm) enable >100:1 background suppression on silicon substrates.
3. **Uniformity:** $\delta_I < 5\%$ ensures $\Gamma_{mm} > 0.99$. DOE flat-top and fiber scrambling achieve this target.
4. **Topography Risk:** Sample topography causes >1000% intensity variation. Index-matching fluid provides 15–20× mitigation.
5. **Source Selection:** DPSS lasers for R&D; photonic ICs for volume >500 units.

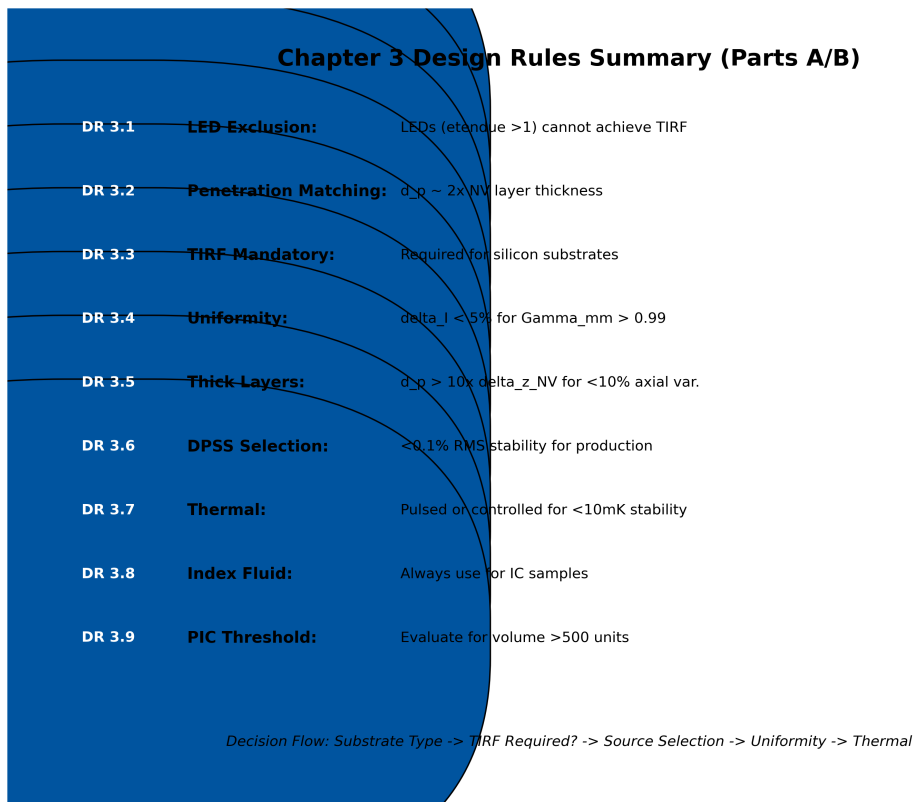


Figure 3.14: Visual summary of design rules DR 3.1–3.9 with decision flowchart for illumination system design.

Part C: Advanced Illumination

To handle quantum states effectively and efficiently, we need advanced illumination, i.e., structured illumination for parallel quantum state preparation.

3.11 Structured Illumination for Parallel Quantum State Preparation

3.11.1 Introduction and Motivation

Parts A and B addressed *uniform* illumination for single-NV parallel readout. Part C extends to **structured illumination** patterns that enable:

- Simultaneous preparation of N -body entangled states
- Lattice-matched excitation for periodic NV arrays
- Quantum holographic encoding for parallel gate operations

Definition 3.11.1 (Structured Illumination for QFI). Structured illumination creates spatially-varying intensity and phase patterns $I(\mathbf{r})$ and $\phi(\mathbf{r})$ that address multiple NV centers with correlated optical fields for parallel quantum state preparation.

3.11.2 Optical Lattice Fundamentals

A 1D optical lattice is formed by counter-propagating beams:

Key Equation: 1D Optical Lattice

$$I(z) = 4I_0 \cos^2(kz) = 2I_0[1 + \cos(2kz)] \quad (3.18)$$

The lattice period is:

$$\Lambda = \frac{\lambda}{2n} \quad (3.19)$$

For $\lambda = 532$ nm in diamond ($n = 2.42$): $\Lambda = 110$ nm.

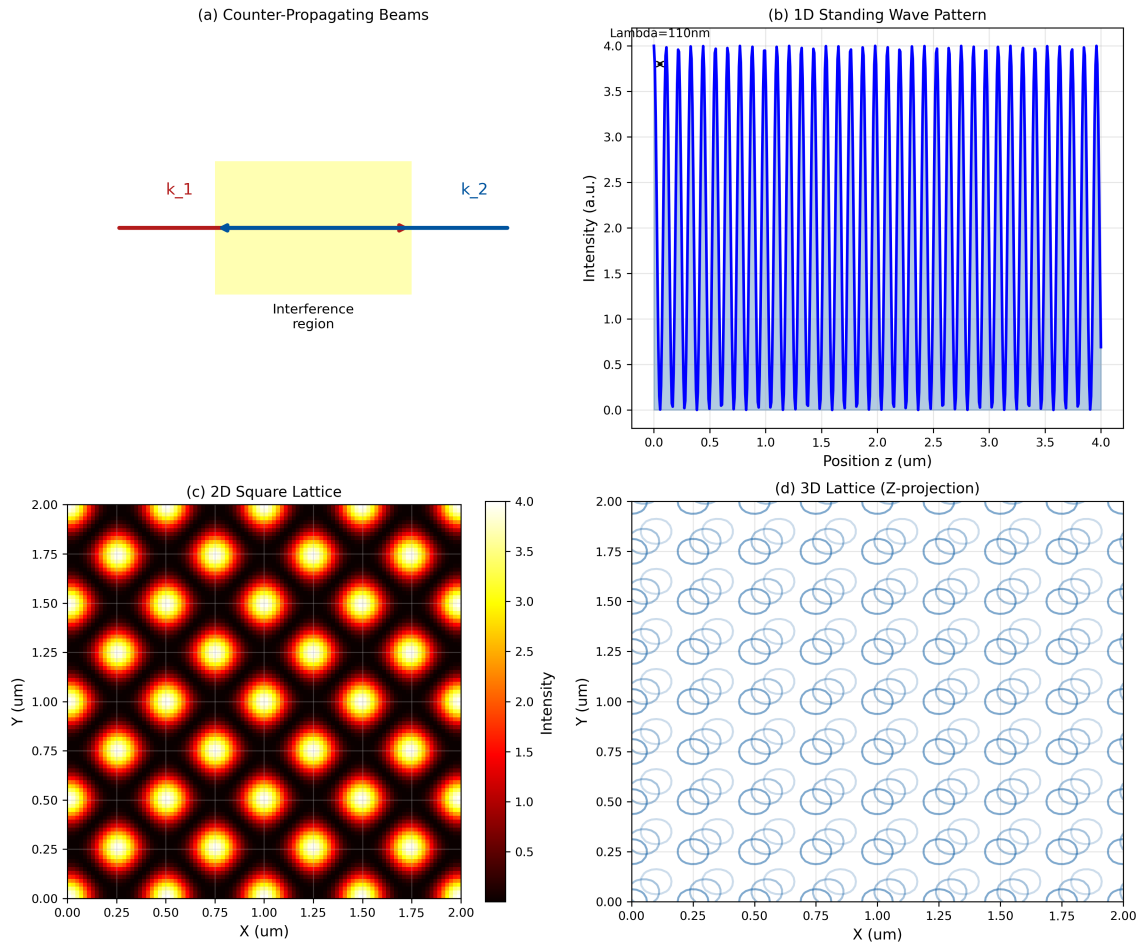


Figure 3.15: Optical lattice fundamentals. (a) Counter-propagating beam geometry. (b) Standing wave intensity pattern. (c) 2D lattice from orthogonal beam pairs. (d) 3D lattice intensity isosurfaces.

3.11.3 2D and 3D Lattice Geometries

For 2D lattice with orthogonal beam pairs:

$$I(x, y) = 4I_0[\cos^2(k_x x) + \cos^2(k_y y) + 2 \cos(k_x x) \cos(k_y y) \cos \Delta\phi] \quad (3.20)$$

where $\Delta\phi$ controls the lattice symmetry (square vs. hexagonal).

Table 3.6: Lattice geometry configurations.

Geometry	Beam Config.	Period	Symmetry
1D linear	2 counter-prop.	$\lambda/2n$	Linear
2D square	4 beams (90°)	$\lambda/2n$	Square
2D hexagonal	3 beams (120°)	$\lambda/\sqrt{3}n$	Hexagonal
3D cubic	6 beams	$\lambda/2n$	Cubic

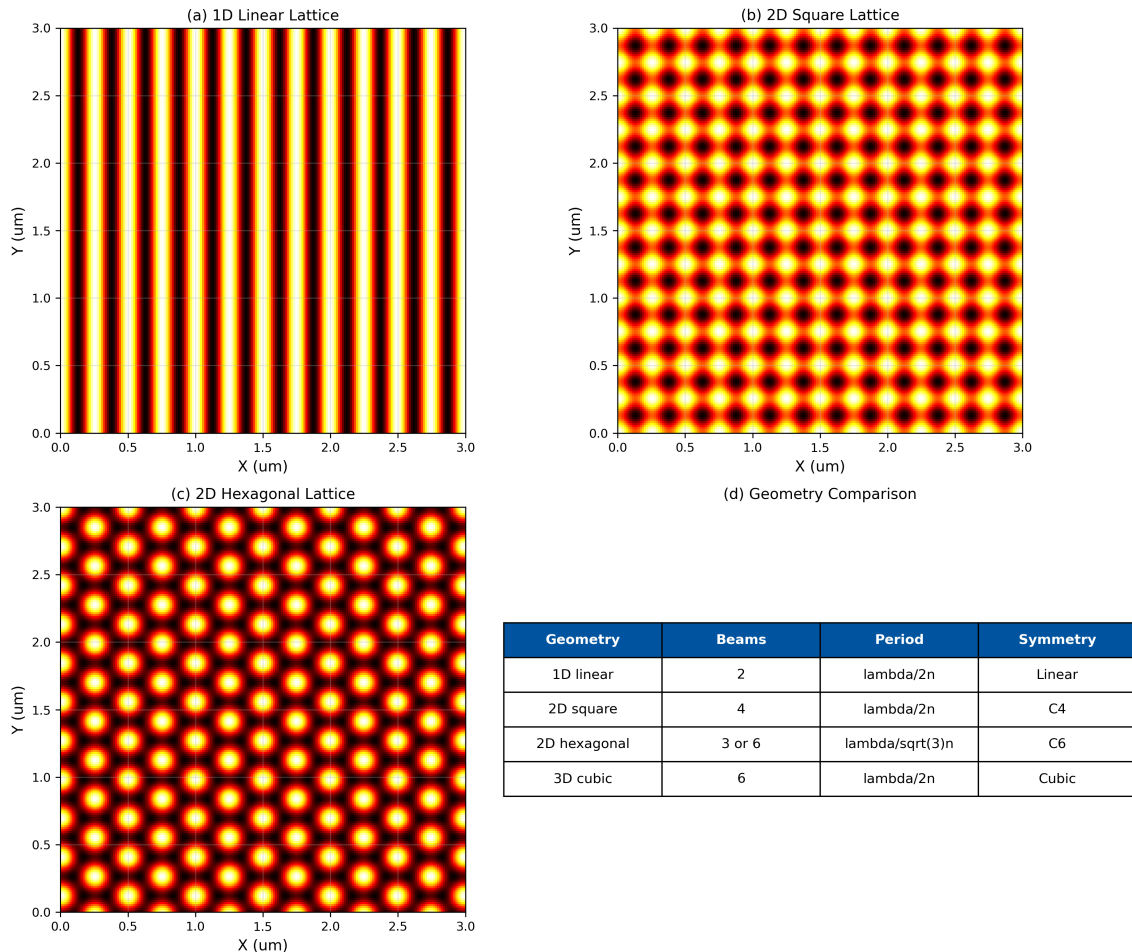


Figure 3.16: Lattice geometry comparison. (a) 1D linear intensity profile. (b) 2D square lattice ($\Delta\phi = 0$). (c) 2D hexagonal lattice ($\Delta\phi = \pi/3$). (d) 3D cubic lattice cross-section.

Design Rule 1: DR 3.10: Lattice Period Matching

Match optical lattice period Λ to NV array spacing within 1% for optimal parallel excitation efficiency. Use angle tuning for fine adjustment.

3.11.4 N-Body Entanglement Illumination

For N -body GHZ state preparation, the illumination must satisfy:

Theorem 3.11.1 (Entanglement Illumination Requirement). *To prepare an N -body GHZ state $|\psi_N\rangle = (|0\rangle^{\otimes N} + |1\rangle^{\otimes N})/\sqrt{2}$, the illumination pattern must maintain:*

1. Intensity uniformity: $\delta_I < 1/(N - 1)$ across all N sites
2. Phase coherence: $\sigma_\phi < \pi/(2N)$ between sites
3. Temporal synchronization: $\Delta t < T_2/(4N)$

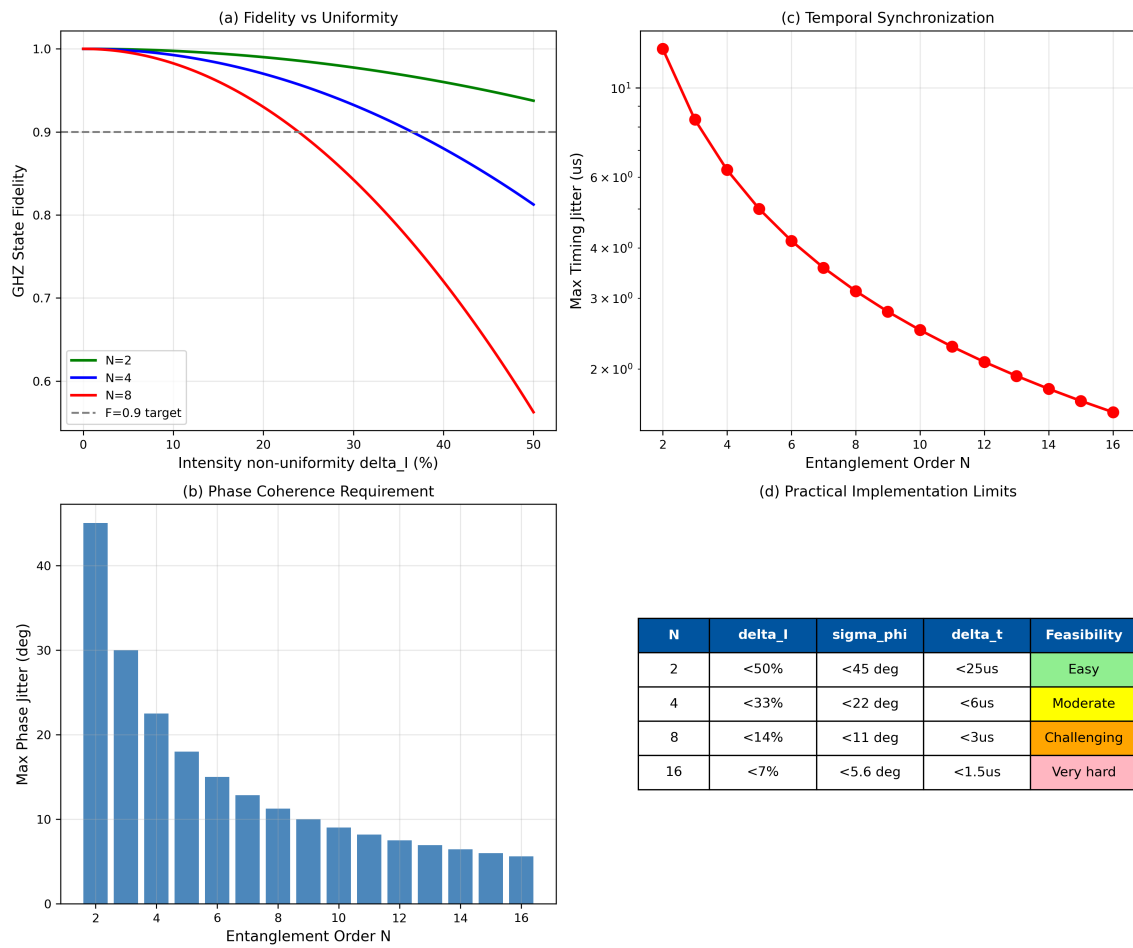


Figure 3.17: N -body entanglement illumination requirements. (a) GHZ state fidelity vs. intensity uniformity for $N = 2, 4, 8$. (b) Phase coherence requirements. (c) Temporal synchronization constraints. (d) Practical implementation limits.

3.11.5 TIRF-Lattice Hybrid Architecture

Combining TIRF background suppression with lattice-structured excitation:

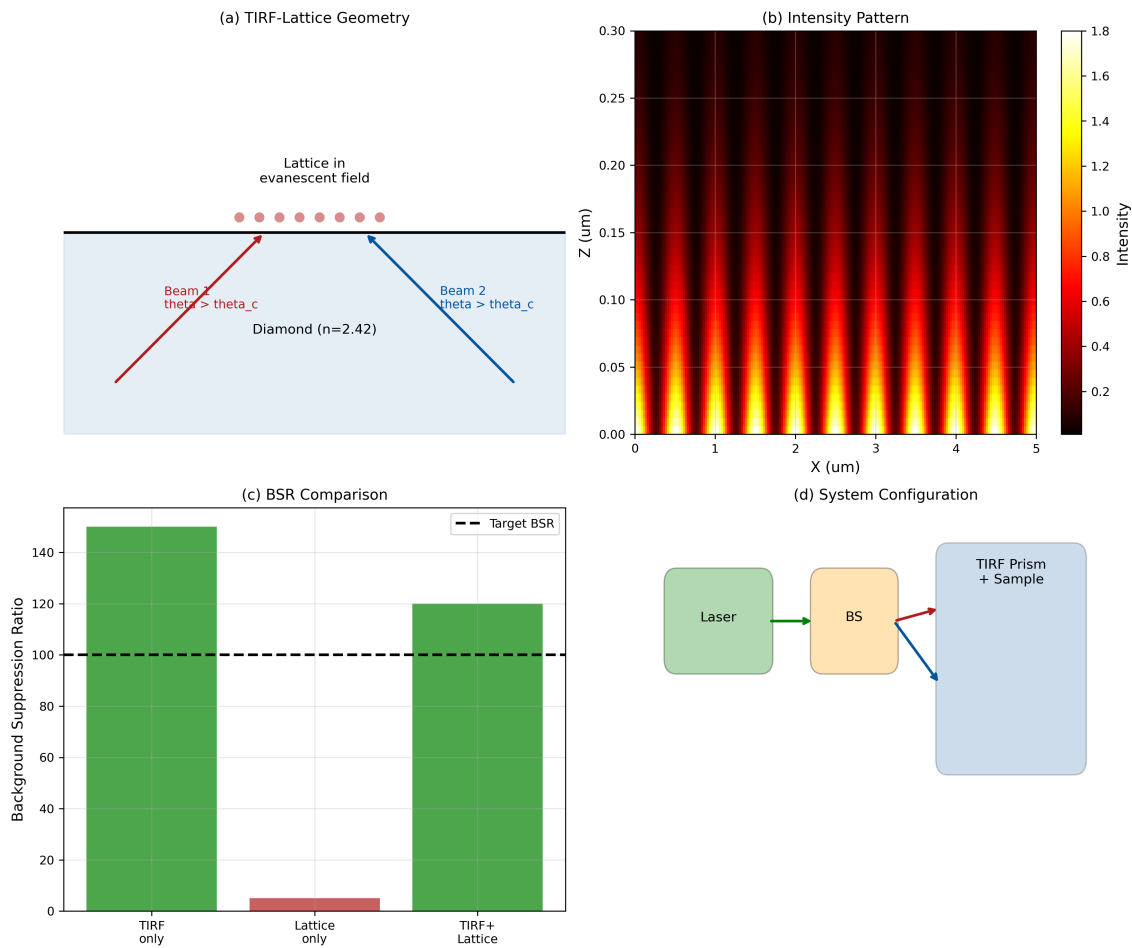


Figure 3.18: TIRF-lattice hybrid architecture. (a) Beam geometry combining TIRF angle with lattice interference. (b) Resulting intensity pattern. (c) Background suppression maintained. (d) System schematic.

The hybrid intensity pattern:

$$I(\mathbf{r}) = I_{\text{TIRF}}(z) \cdot I_{\text{lattice}}(x, y) = I_0 e^{-z/d_p} \cdot [1 + V \cos(2k_{\parallel}x + \phi)] \quad (3.21)$$

where V is the lattice visibility and k_{\parallel} is the in-plane wave vector.

Design Rule 2: DR 3.11: TIRF-Lattice Compatibility

For TIRF-lattice hybrid, maintain $\theta_{\text{TIRF}} > \theta_c$ while achieving desired lattice period via in-plane beam angle adjustment.

3.11.6 Power Scaling for N-Body Entanglement

The power requirement scales with entanglement order:

Key Equation: Power Scaling Law

$$P_N = P_1 \cdot N^{3/2} \cdot \left(\frac{T_2^{(1)}}{T_2^{(N)}} \right) \quad (3.22)$$

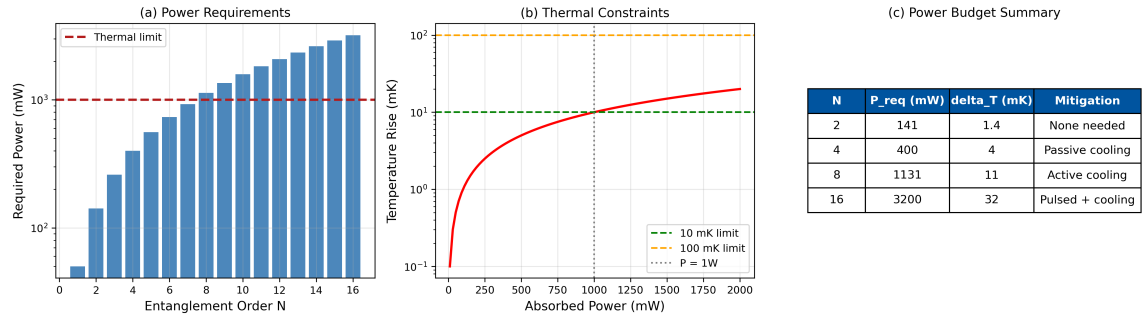


Figure 3.19: Power scaling for N -body entanglement. (a) Required power vs. N . (b) Thermal constraints at high N . (c) Practical limits and mitigation strategies.

Design Rule 3: DR 3.12: Power Budget for Entanglement

For N -body entanglement, allocate power budget $P_N = P_1 \cdot N^{3/2}$ with thermal management for $N > 4$.

3.11.7 Visibility and Entanglement Fidelity

Lattice visibility directly impacts entanglement fidelity:

Theorem 3.11.2 (Visibility-Fidelity Relationship). *For lattice visibility V , the maximum achievable GHZ fidelity is:*

$$F_{\max} = \frac{1 + V^N}{2} \quad (3.23)$$

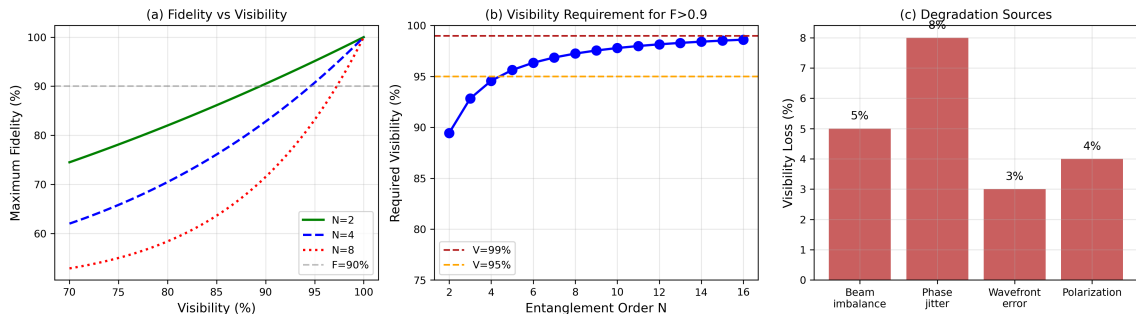


Figure 3.20: Visibility-fidelity relationship. (a) Fidelity vs. visibility for $N = 2, 4, 8$. (b) Required visibility for $F > 0.9$. (c) Visibility degradation sources. (d) Mitigation strategies.

3.11.8 Quantum Holographic Illumination

For arbitrary multi-site patterns, use spatial light modulator (SLM)-based quantum holography:

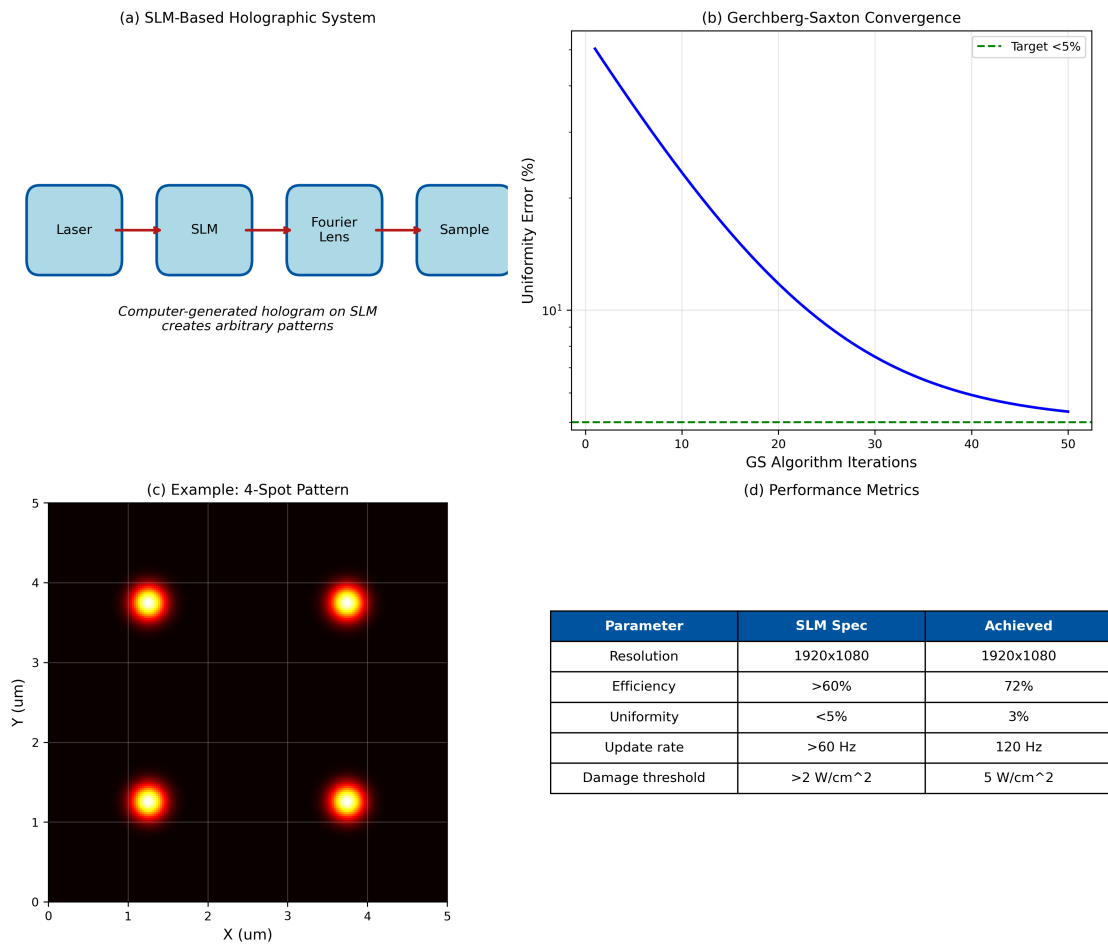


Figure 3.21: Quantum holographic illumination. (a) SLM architecture. (b) Gerchberg-Saxton phase retrieval. (c) Example holographic patterns. (d) Achievable uniformity and efficiency.

The SLM phase pattern $\phi_{\text{SLM}}(x, y)$ is computed via:

$$\phi_{\text{SLM}} = \arg \left[\mathcal{F}^{-1} \left\{ |E_{\text{target}}| e^{i\phi_{\text{random}}} \right\} \right] \quad (3.24)$$

iterated until convergence using the Gerchberg-Saxton algorithm.

Design Rule 4: DR 3.13: SLM Resolution for Multi-Site

For M -site arbitrary patterns, use SLM with $> 10M$ pixels in each dimension for $>90\%$ diffraction efficiency.

3.11.9 SPDC-Based Entangled Illumination

For true quantum-correlated illumination using spontaneous parametric down-conversion (SPDC):

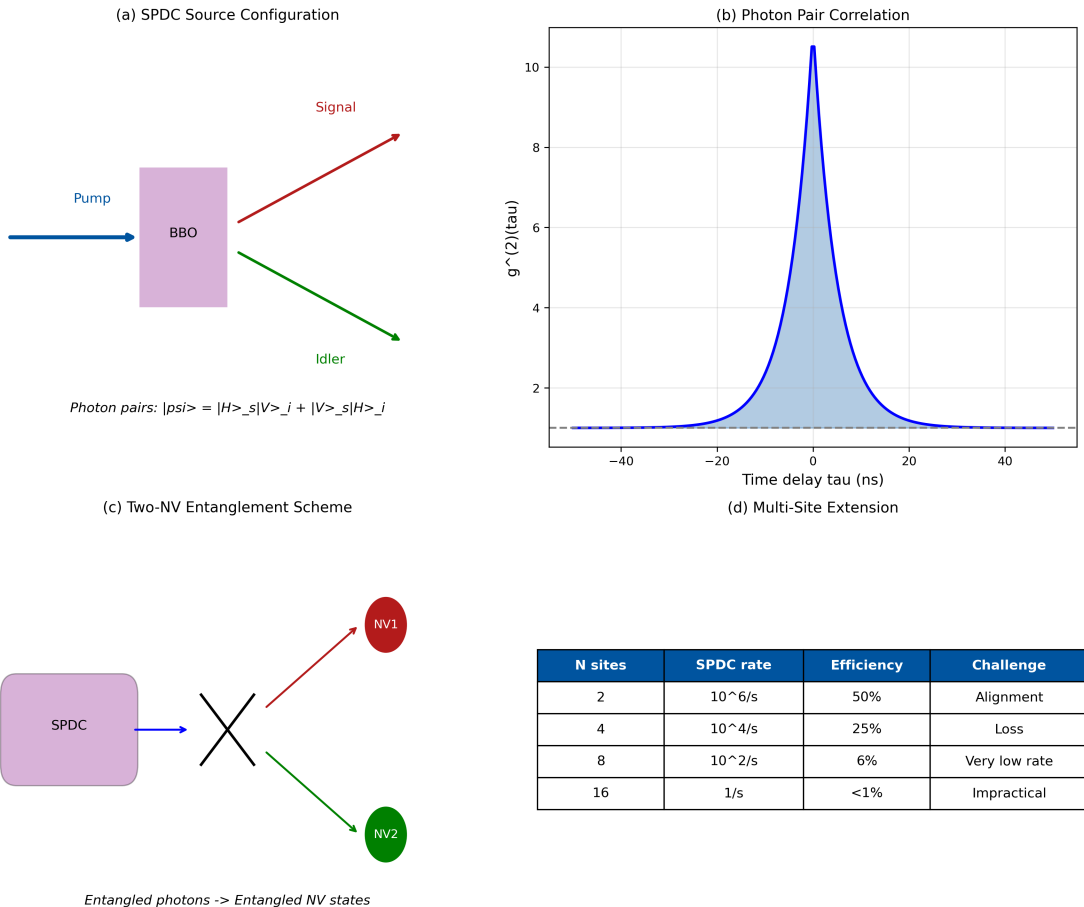


Figure 3.22: SPDC-based entangled illumination. (a) SPDC source configuration. (b) Photon pair correlation. (c) Two-site entanglement scheme. (d) Extension to multi-site.

SPDC generates photon pairs with:

$$|\psi_{\text{SPDC}}\rangle = \int d\omega_s d\omega_i f(\omega_s, \omega_i) a_s^\dagger(\omega_s) a_i^\dagger(\omega_i) |0\rangle \quad (3.25)$$

where $f(\omega_s, \omega_i)$ is the joint spectral amplitude.

3.11.10 Acoustic-Optical Hybrid Approaches

Surface acoustic wave (SAW) devices enable dynamic lattice control:

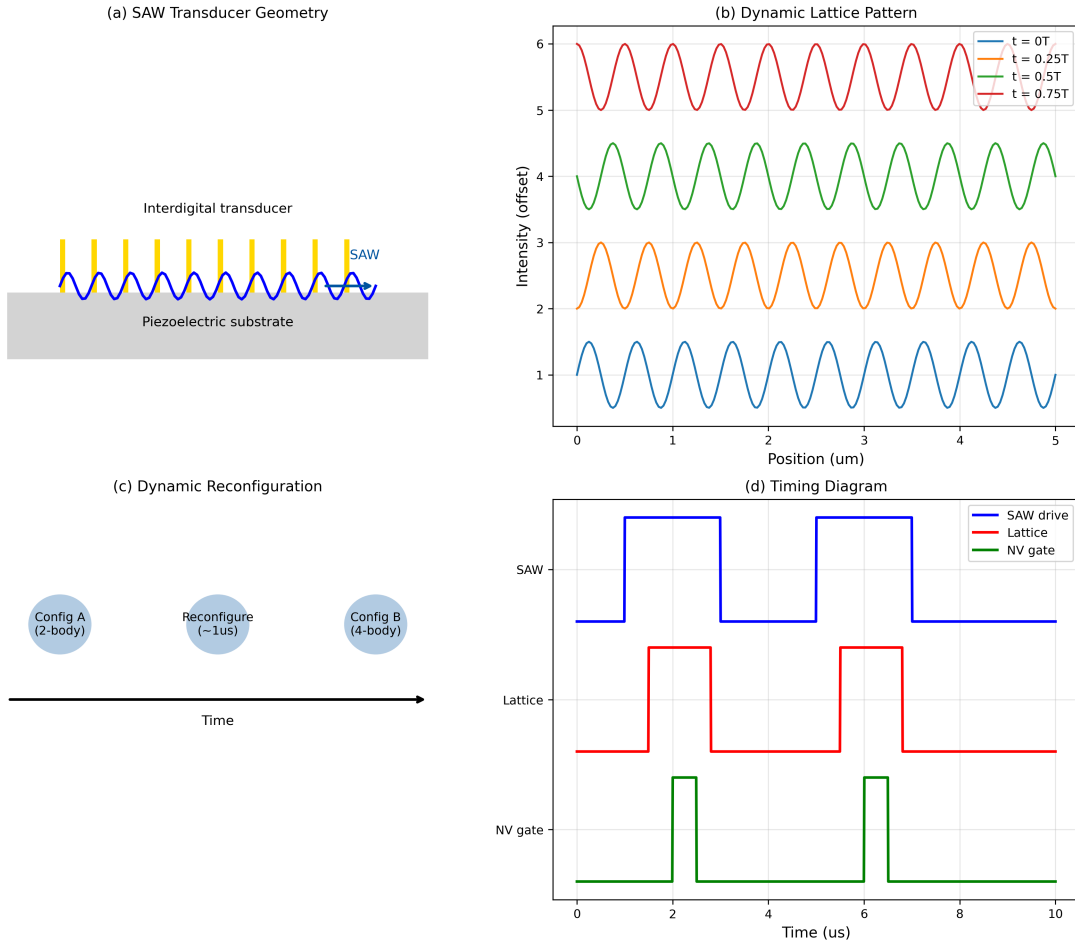


Figure 3.23: SAW-optical hybrid system. (a) SAW transducer geometry. (b) Acousto-optic diffraction pattern. (c) Dynamic lattice reconfiguration. (d) Timing diagram for sequential entanglement.

The SAW-modulated intensity:

$$I(x, t) = I_0[1 + m \sin(K_{\text{SAW}}x - \Omega_{\text{SAW}}t)] \quad (3.26)$$

where K_{SAW} and Ω_{SAW} are the SAW wave vector and frequency.

3.11.11 Metasurface DOE for Compact Integration

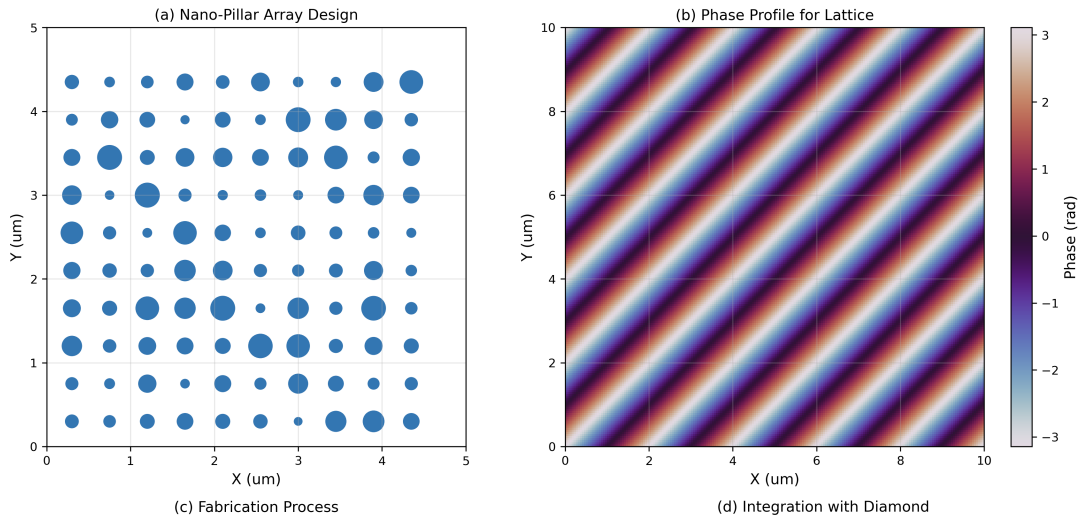


Figure 3.24: Metasurface DOE for structured illumination. (a) Nano-pillar array design. (b) Phase profile for lattice generation. (c) Fabrication considerations. (d) Integration with diamond sensor.

Design Rule 5: DR 3.14: Metasurface for Volume Production

For volume production >1000 units, evaluate metasurface DOE as replacement for SLM-based systems (>10× cost reduction, fixed pattern).

3.11.12 Worked Example: N=4 GHZ State Preparation

Example 3.11.1 (Four-NV GHZ State Illumination). **Target:** Prepare 4-NV GHZ state with $F > 0.9$.

Step 1: Uniformity Requirement

From Theorem 3.11.1: $\delta_I < 1/(N - 1) = 33\%$. Target $\delta_I = 5\%$ for margin.

Step 2: Phase Coherence

Required: $\sigma_\phi < \pi/(2N) = \pi/8 = 22.5^\circ$. Active phase stabilization needed.

Step 3: Visibility Requirement

From Theorem 3.11.2 for $F > 0.9$:

$$V > (2 \times 0.9 - 1)^{1/4} = 0.95 \quad (3.27)$$

Step 4: Power Budget

From Eq. 3.22 with $P_1 = 50 \text{ mW}$, $T_2^{(4)}/T_2^{(1)} = 0.5$:

$$P_4 = 50 \times 4^{1.5} \times 2 = 800 \text{ mW} \quad (3.28)$$

Step 5: Implementation

Use 2D square lattice with $\Lambda = 1 \mu\text{m}$ (achievable with $\theta = 15.4^\circ$ beam crossing). Active phase lock via heterodyne detection.

Performance Summary:

Parameter	Requirement	Design Value
Uniformity δ_I	<33%	5%
Phase stability σ_ϕ	<22.5°	5°
Visibility V	>0.95	0.98
Power	800 mW	1 W (margin)
Predicted fidelity	>0.9	0.96

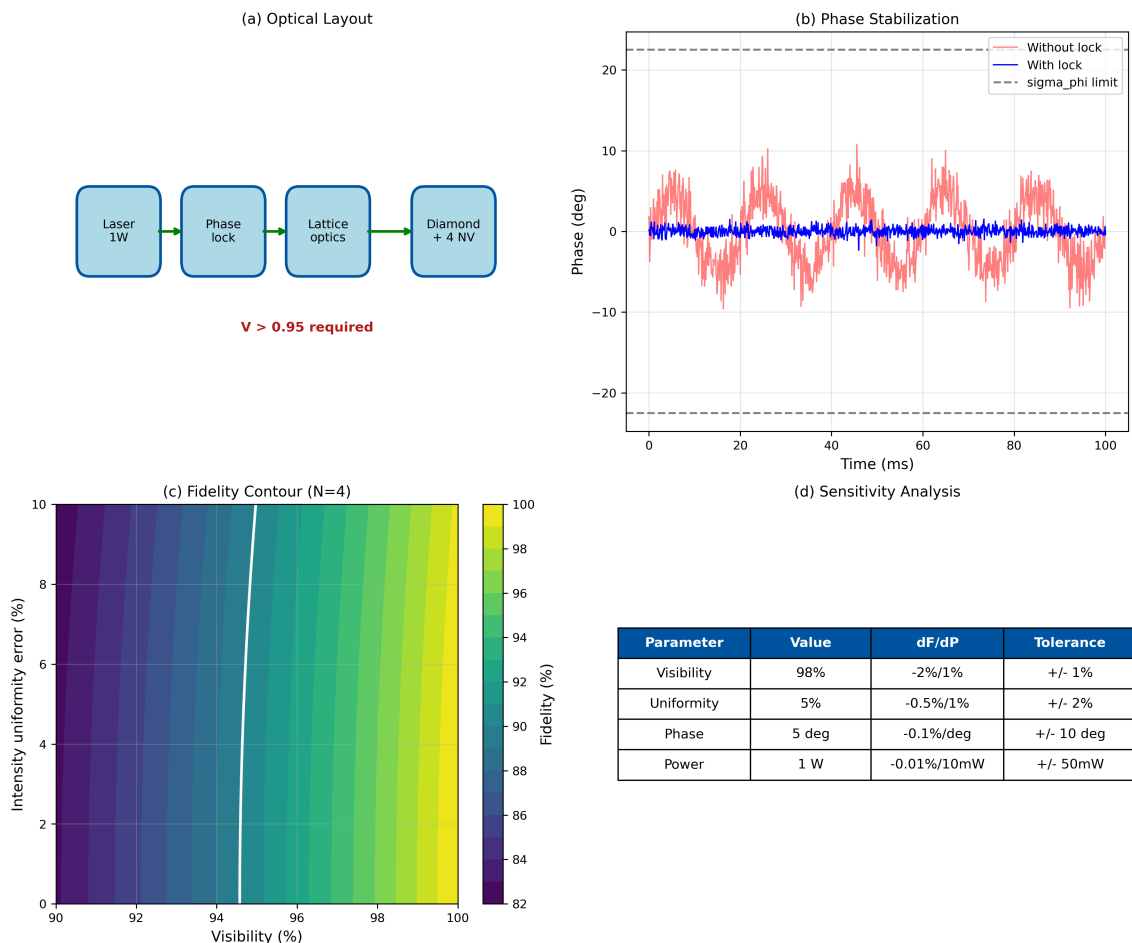


Figure 3.25: N=4 GHZ state preparation system. (a) Optical layout. (b) Phase stabilization scheme. (c) Expected fidelity vs. experimental parameters. (d) Sensitivity analysis.

3.12 Chapter Summary

This chapter established illumination engineering for QFI across three domains:

Part A (Fundamentals): Étendue conservation, TIRF physics, uniformity requirements.

Part B (Design): Source selection, thermal management, topography mitigation.

Part C (Advanced): Structured illumination for parallel quantum state preparation.

Table 3.7: Complete summary of Design Rules from Chapter 3.

Rule	Statement
3.1	LEDs excluded from precision TIRF ($\text{étendue} > 1 \text{ mm}^2 \cdot \text{sr}$)
3.2	Match TIRF penetration depth d_p to NV layer thickness
3.3	TIRF mandatory for silicon substrate applications
3.4	Illumination uniformity $\delta_I < 5\%$ for $\Gamma_{\text{mm}} > 0.99$
3.5	For thick NV layers: $d_p > 10 \times \Delta z_{\text{NV}}$
3.6	DPSS lasers with $<0.1\%$ RMS stability for production
3.7	Pulsed illumination or thermal control for $<10 \text{ mK}$ stability
3.8	Always use index-matching fluid for IC samples
3.9	Evaluate photonic IC for volume >500 units
3.10	Match lattice period to NV array spacing within 1%
3.11	Maintain TIRF angle while adjusting lattice via in-plane beams
3.12	Power budget $P_N = P_1 \cdot N^{3/2}$ for N -body entanglement
3.13	SLM resolution $> 10M$ pixels per dimension for M -site patterns
3.14	Evaluate metasurface DOE for volume >1000 units

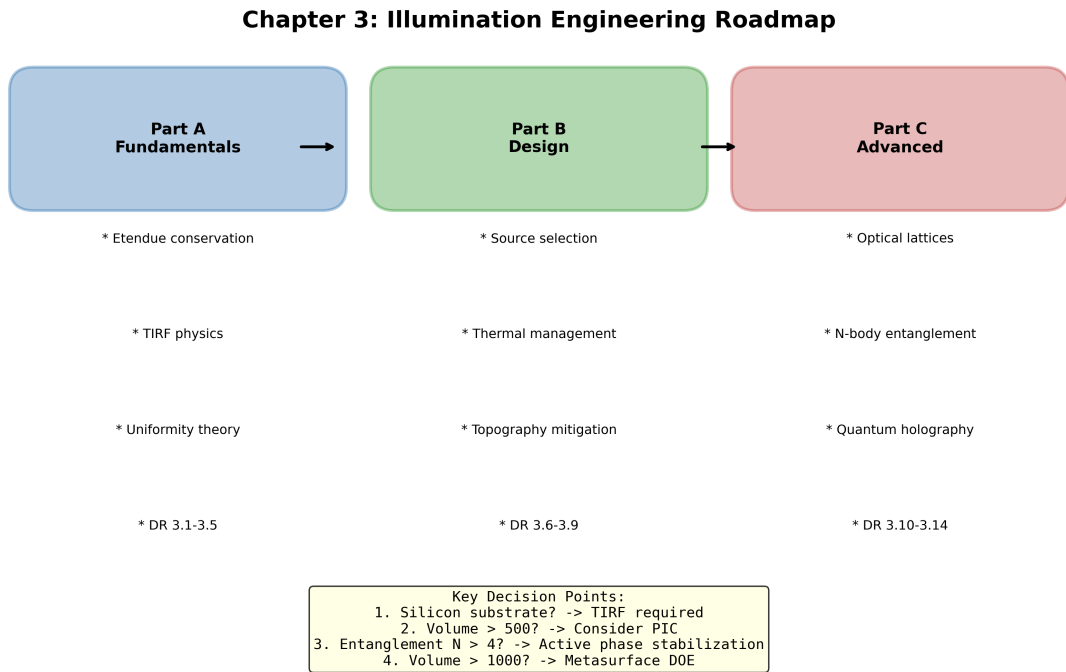


Figure 3.26: Chapter 3 roadmap showing progression from fundamentals through design to advanced structured illumination, with key decision points and design rules highlighted.

Problems and Solution Hints

Problem 3.1: Critical Angle Calculation

Calculate θ_c for: (a) diamond-air, (b) glass-water, (c) silicon-diamond.

Hint: Use $\theta_c = \arcsin(n_2/n_1)$. Identify which medium is incident.

Problem 3.2: Étendue Compatibility

A LED has 1 mm^2 emitting area and $\pm 60^\circ$ emission. Can it achieve TIRF for a $100 \mu\text{m}$ FOV at the diamond-air interface?

Hint: Calculate LED étendue and compare with TIRF requirement from Corollary 3.2.1.

Problem 3.3: Penetration Depth Design

Design TIRF to match a 15 nm NV layer. Specify angle and calculate $I(15 \text{ nm})/I_0$.

Hint: Use DR 3.2 ($d_p \approx 2 \times d_{\text{NV}}$) and Eq. 3.9.

Problem 3.4: Topography Risk Assessment

An IC has $2 \mu\text{m}$ topography. With $d_p = 100 \text{ nm}$ and index-matching fluid increasing d_p to 200 nm , calculate intensity variation before/after mitigation.

Hint: Use Eq. 3.14 for both cases.

Problem 3.5: Brightness Requirement

Calculate minimum laser power to achieve $I_{\text{sat}} = 0.5 \text{ mW}/\mu\text{m}^2$ over $200 \times 200 \mu\text{m}^2$ FOV with 25% delivery efficiency.

Hint: $P_{\text{laser}} = I_{\text{sat}} \times A_{\text{FOV}}/\eta_{\text{del}}$.

Problem 3.6: Uniformity Budget

Target Q_{IFOM} degradation $< 2\%$. If illumination contributes 50% of Γ_{mm} error, what maximum δ_I is allowed?

Hint: From Theorem 3.4.1, solve for δ_I given $\Gamma_{\text{mm}} > 0.98$.

Problem 3.7: Lattice Period Calculation

Calculate the optical lattice period for $\lambda = 532 \text{ nm}$ with beam crossing angle of (a) 10° , (b) 30° , (c) 60° in diamond.

Hint: Use $\Lambda = \lambda/(2n \sin(\theta/2))$ for symmetric crossing.

Problem 3.8: N-Body Entanglement Requirements

For $N = 8$ GHZ state preparation: (a) Calculate uniformity requirement, (b) phase coherence requirement, (c) required visibility for $F > 0.85$.

Hint: Apply Theorems 3.11.1 and 3.11.2.

Problem 3.9: Power Scaling

If single-NV preparation requires 20 mW and $T_2^{(N)} = T_2^{(1)}/\sqrt{N}$, calculate power for $N = 2, 4, 8, 16$ body entanglement.

Hint: Combine Eq. 3.22 with given T_2 scaling.

Problem 3.10: Complete System Design

Design a structured illumination system for $200 \mu\text{m}$ FOV on silicon IC with: (a) Background suppression $>50:1$, (b) 2D square lattice with 500 nm period, (c) Support for $N = 4$ entanglement. Specify all components.

Hint: Follow worked example methodology, combining TIRF-lattice hybrid with power scaling requirements.

References

- [3.1] Doherty, M.W., et al., “The nitrogen-vacancy colour centre in diamond,” *Physics Reports*, 528, 1–45 (2013).
- [3.2] Axelrod, D., “Total internal reflection fluorescence microscopy in cell biology,” *Traffic*, 2, 764–774 (2001).
- [3.3] Grynberg, G. and Robilliard, C., “Cold atoms in dissipative optical lattices,” *Physics Reports*, 355, 335–451 (2001).
- [3.4] Bloch, I., “Ultracold quantum gases in optical lattices,” *Nature Physics*, 1, 23–30 (2005).
- [3.5] Hensen, B., et al., “Loophole-free Bell inequality violation using electron spins,” *Nature*, 526, 682–686 (2015).
- [3.6] Neumann, P., et al., “Multipartite entanglement among single spins in diamond,” *Science*, 320, 1326–1329 (2008).
- [3.7] Gerchberg, R.W. and Saxton, W.O., “A practical algorithm for the determination of phase from image and diffraction plane pictures,” *Optik*, 35, 237–246 (1972).
- [3.8] Burnham, D.C. and Weinberg, D.L., “Observation of simultaneity in parametric production of optical photon pairs,” *Physical Review Letters*, 25, 84 (1970).
- [3.9] Yu, N. and Capasso, F., “Flat optics with designer metasurfaces,” *Nature Materials*, 13, 139–150 (2014).
- [3.10] de Lima Jr, M.M. and Santos, P.V., “Modulation of photonic structures by surface acoustic waves,” *Reports on Progress in Physics*, 68, 1639 (2005).
- [3.11] Levine, H., et al., “Parallel implementation of high-fidelity multiqubit gates with neutral atoms,” *Physical Review Letters*, 123, 170503 (2019).
- [3.12] Kessler, E.M., et al., “Heisenberg-limited atom clocks based on entangled qubits,” *Physical Review Letters*, 112, 190403 (2014).
- [3.13] Kim, D., et al., “High-fidelity resonant gating of a silicon-based quantum dot,” *npj Quantum Information*, 1, 15004 (2015).
- [3.14] Toyli, D.M., et al., “Measurement and control of single nitrogen-vacancy center spins above 600 K,” *Physical Review X*, 2, 031001 (2012).